Electron-impact total ionization cross sections of CF_4, C_2F_6, and C_3F_8

H. Nishimura[a)]
Department of Physics, Niigata University, Niigata 950-21, Japan

Winifred M. Huo
NASA Ames Research Center, Moffet Field, California 94035-1000

M. A. Ali
Department of Chemistry, Howard University, Washington, District of Columbia 20059

Yong-Ki Kim[b)]
National Institute of Standards and Technology, Gaithersburg, Maryland 20899-0001

(Received 27 May 1998; accepted 18 November 1998)

Both theoretical and experimental electron-impact total ionization cross sections of CF_4, C_2F_6, and C_3F_8 are presented. The experimental cross sections have been measured as a function of incident electron energy T from threshold to 3 keV. A parallel plate condenser type apparatus was used. The molecular polarizability for C_3F_8 was empirically estimated to be $\alpha = 10.6\ \text{Å}^3 \pm 0.8\ \text{Å}^3$. Theoretical cross sections calculated from the binary-encounter-Bethe (BEB) method, which combines a modified form of the Mott cross section and the Bethe cross section, are compared with the experimental cross sections. The BEB cross sections calculated from correlated molecular wave functions with theoretical estimates for multiple ionization are about 10% higher than the experimental data at the peak for CF_4, while they are in excellent agreement with the experimental data for C_2F_6 and C_3F_8. Our analysis shows that the BEB theory implicitly includes part of neutral dissociation, such as $CF_4 \rightarrow CF_3 + F$, and hence tends to be an upper limit to the total ionization cross section. We found that the difference between our best theory for CF_4 and the present experimental cross section exhibits a remarkable similarity to the shape of the recently measured cross section for neutral dissociation, though there is no *a priori* reason for the similarity. Owing to the large number of bound electrons, the correlation included in our wave functions for C_2F_6 and C_3F_8 is more limited than for CF_4. Hence, we believe that for these two molecules the calculated cross sections are lower than the true BEB values, in spite of the apparent excellent agreement between the theory and the experiment.
[S0021-9606(99)01608-6]

I. INTRODUCTION

In the semiconductor industry, simple fluorocarbon molecules have been used widely for plasma processing. To unravel the elementary processes in the etching plasma, a number of measurements of electron-impact total ionization cross sections σ_i, partial ionization cross sections σ_p, and neutral dissociation cross sections σ_{nd}, have been reported. Beran and Kevan[1] measured σ_i of CF_4, C_2F_6, and C_3F_8 (at incident electron energy $T = 20$, 35, and 70 eV) with a magnetic mass spectrometer. Stephan *et al.*[2] reported σ_p and σ_i of CF_4 (from threshold to $T = 180$ eV) with a double focusing sector field mass spectrometer. Kurepa[3] obtained σ_i of C_2F_6, C_3F_8, and C_4F_8 (from threshold to $T = 100$ eV) with a parallel plate apparatus similar to the one used by Tate and Smith.[4] Poll and Meichsner[5] measured σ_i and σ_p of CF_4, C_2F_6, C_3F_8, and many other related molecules ($T = 5-125$ eV) with a quadrupole mass spectrometer. Also, Poll *et al.*[6] revised the data by Stephan *et al.*[2] upwards after including the effect of ions with appreciable kinetic energies.

For CF_4, Winters and Inokuti[7] reported the total dissociation cross section σ_{td}, i.e., the sum of dissociative ionization and neutral dissociation cross section σ_{nd} (from threshold to $T = 600$ eV) using an apparatus combined with a quadrupole mass filter and an ionization gauge tube with a titanium getter. Since CF_4 is known to produce very little CF_4^+ by electron impact, σ_{td} measured by Winters and Inokuti[7] for CF_4 is practically the sum of the total ionization cross section and the neutral dissociation cross section, $\sigma_{td} \approx \sigma_i + \sigma_{nd}$. Ma *et al.*[8] measured σ_p and σ_i for CF_4 ($T = 20-500$ eV) with a pulsed electron beam time of flight apparatus. The experimental values by Ma *et al.* were later revised and increased by Bruce and Bonham.[9] Recently Rao and Srivastava[10] reported σ_p and σ_i also for CF_4 (from threshold to $T = 1$ keV) utilizing crossed beam geometry and pulsed extraction technique with a time of flight and a quadrupole mass spectrometer. As seen above, most measurements of σ_i focused on CF_4. However, more information can be obtained from a systematic study of σ_i of perfluoroalkanes. In the experiments mentioned above, each apparatus was operated under its own intrinsic principle and among them only three groups[1,9,10] obtained results in close agreement. This motivated the present experiments which

[a)]Permanent address: 1-13-11, Iwanaridai, Kasugai-shi, 4870033 Japan.
[b)]Electronic mail: kim@atm.nist.gov

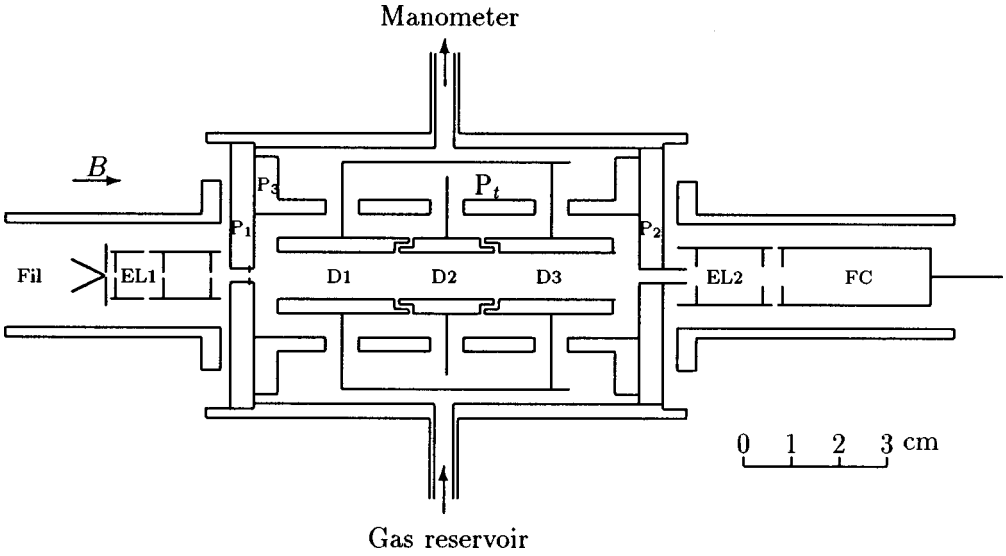

FIG. 1. Schematic diagram of the experimental apparatus.

utilize an apparatus of the Rapp and Englander-Golden[11] type to measure the σ_i of CF_4, C_2F_6, and C_3F_8 over a wide range of T.

On the theory side, there have been numerous efforts to combine the Mott cross section[12] with the Bethe theory[13] since the 1950s.[14–18] However, these attempts involved semiempirical parameters specific to each target atom or molecule and were not easily extendable to large molecules such as C_3F_8 or molecules with no experimental data for either the molecule itself or the constituent atoms. Another semiempirical theory is the ''DM formalism,'' which combines a classical binary-encounter theory with an additivity rule. In the DM formalism for molecules,[19] semiempirical weights are introduced for each atomic orbital of the constituent atoms of a molecule, while additional molecular orbital factors are assigned using the Mulliken population analysis.

Kim and Rudd[20] developed a theory of σ_i for electron-impact ionization of molecules by combining a modified form of the Mott cross section at low T and the Bethe theory for high T. The theory by Kim and Rudd does not involve empirical parameters specific to each target molecule unlike past attempts. The simplest form of σ_i proposed by Kim and Rudd, referred to as the binary-encounter-Bethe (BEB) model, uses all theoretical data from the ground-state wave function, except for the lowest ionization potential (IP), for which an experimental vertical IP, if available, is used to match the experimental threshold.

Kim and co-workers[21–25] have shown that molecular wave functions of modest accuracy (Hartree–Fock or inferior) can produce σ_i in good agreement (15% or better at the peak) with available experimental data from threshold to $T \sim 5$ keV for a wide range of molecules and radicals, such as H_2 and SF_6. However, there is a need to find out how the BEB model will perform if a correlated wave function is used. In this article, we compare the BEB cross sections calculated from both correlated and uncorrelated ground-state wave functions, and compare them to the experiments.

As will be presented later, the use of a correlated wave function resulted in an unexpected bonus. The BEB theory assumes all energy transfers above the orbital binding energies would result in an inelastic collision (ionizing or dissociative), while experiments on ionization cross sections measure only the actual ions produced. Therefore, the difference between the BEB theory and the measured total ionization cross section, which we shall refer to as the ''excess'' BEB cross section, should be related to the neutral dissociation cross section, σ_{nd}. Indeed, we found that this was the case for CF_4 because we were able to obtain a good correlated wave function for the molecule. However, the exact relation between the excess BEB cross section and the true σ_{nd} is unclear at present and requires further investigation.

We describe experimental procedures in Sec. II, outline the BEB theory in Sec. III, and compare our theory and experiment to other available experimental data in Sec. IV. Our conclusions are presented in Sec. V.

II. EXPERIMENT

A. Apparatus

The apparatus used in this study has already been reported elsewhere;[26] it is similar to that used by Rapp and Englander-Golden.[11] Therefore, only the changes in design from the instrument reported earlier[26] will be presented. This experiment was performed at the Niigata University. A schematic diagram is shown in Fig. 1.

(a) The temperature of the target gas is determined from the temperature of the plate P3 which is monitored with a platinum thin film device attached on the plate instead of a calibrated thermistor. The reading of the manometer is corrected at each pressure measurement taking into account the thermal transpiration effect caused by the difference of temperature of the manometer and that of the collision cell.

(b) An element EL2 with appropriate retarding potential is attached in front of a Faraday cup to remove slow electrons among the transmitted electrons.

(c) Measurement of σ_i was made in the pressure range of 20–47 Pa (0.15–0.35 mTorr) for target molecules.

TABLE I. Vertical first ionization potentials in eV. From Ref. 27.

CF_4	C_2F_6	C_3F_8
16.20	14.48	13.70

The rest of the apparatus is the same as in the previous paper.[26] Briefly, all elements are assembled and placed in a stainless steel vacuum chamber and evacuated below 0.133 Pa (1×10^{-6} Torr) by a 6-inch oil diffusion pump with a liquid nitrogen trap.

A coaxial uniform magnetic field (0.047 T) is applied to this apparatus for the confinement of electrons. The intensity of the electron beam is kept below 1 nA. For the detection of ions produced in the collision cell (8.6 cm in the inside measurement), appropriate ion drawout field is applied between the ion collection plates D1, D2, and D3.

The energy width [full width at half maximum (FWHM)] of electrons emitted from directly heated rhenium hair pin type filament is estimated to be 0.5 eV from the ion current distribution measured as function of electron energy near threshold.

B. Procedure

The measured ion current per unit electron path length I_i is given as

$$I_i = I_e\, n\, l\, \sigma_i, \tag{1}$$

where I_e is the electron beam current passing through the space defined by D2, n is the target gas density, and l is the effective electron path length. At each electron energy two measurements are carried out successively for low and high target gas pressure. The suffix 1 is given for the former and the suffix 2 is given for the latter. As the exact measurement of the electron current near D2 is difficult, the electron current is defined in this study as

$$I_e = \frac{I_{e1}+I_{e2}}{2}. \tag{2}$$

Therefore, Eq. (2) is rewritten as

$$\sigma_i = 2\frac{I_{i2}-I_{i1}}{l(I_{e1}+I_{e2})(n_2-n_1)}. \tag{3}$$

For the electron energy calibration, the behavior of σ_i near threshold is compared with the available data for ionization potential. Table I lists the ionization potentials used in the present study.[27]

For complete collection of ions, σ_i is tested as a function of ion drawout fields (V/cm). As an example, results for C_2F_6 are shown in Fig. 2. The other molecules also showed similar behavior. Based on these results, in our measurement the applied drawout fields on D1, D2, and D3 were 10 V/cm for $T<30$ eV, 26 V/cm for 35 eV $<T<90$ eV and 46 V/cm for $T>100$ eV. The mid-plane of the ion collection plate is kept at the ground potential so that the incident electron energy would not shift after the incident electron leaves the collision cell.

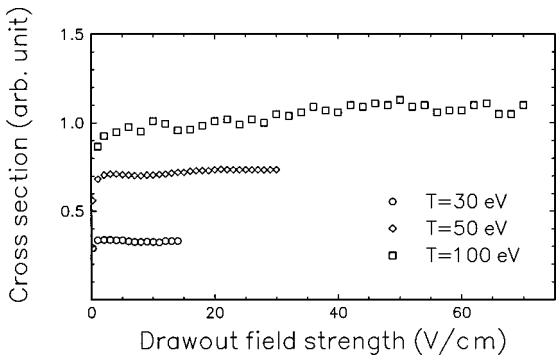

FIG. 2. Ion collection efficiency at $T=30$, 50, and 100 eV vs drawout field in V/cm.

The target gas pressure dependence of σ_i was tested for these three molecules at $T=100$ eV. Results are shown in Fig. 3. No pressure dependence of σ_i was found below 47 Pa (3.5×10^{-4} Torr) for these gases in the collision cell.

III. THEORY

A. Ionization cross section

Our theory for electron-impact ionization starts from the binary-encounter-dipole (BED) model,[20] which combines a modified form of the Mott theory[12] at low T and the Bethe theory[13] at high T by requiring the ionization cross section itself and the corresponding stopping cross section to satisfy the asymptotic behavior of the Bethe theory at high T. The stopping cross section is the integral of the product of the energy transfer from the incident electron to the target and the corresponding differential ionization cross section. The BED model requires explicit knowledge of the continuum dipole oscillator strength, df/dE where E is the photon energy, for each molecular orbital in the initial state of the target molecule. We can then integrate the differential cross section and determine the total ionization cross section, σ_i, for each molecular orbital with its binding energy B, kinetic energy $U=\langle \mathbf{p}^2/2m\rangle$, and electron occupation number N.[20]

Before proceeding further, we first define two quantities, m^2_{ion} and Q for individual molecular orbitals. They are related to df/dE by

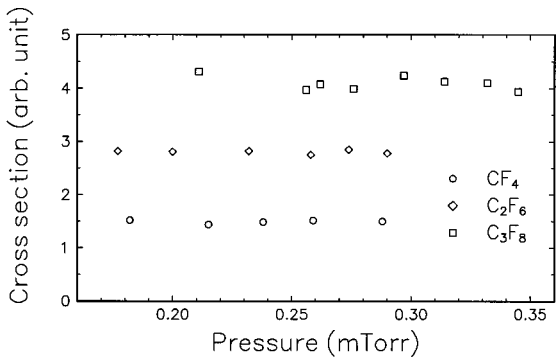

FIG. 3. Pressure dependence of total ionization cross section σ_i at $T=100$ eV.

$$m_{\rm ion}^2=\frac{R}{B}\int_0^\infty \frac{1}{w+1}\frac{df(w)}{dw}dw, \tag{4}$$

$$Q=\frac{2Bm_{\rm ion}^2}{NR}, \tag{5}$$

with $w=W/B$, W being the kinetic energy of the ejected electron. With this notation, the photon energy E becomes $E=B+W$.

For most molecules, df/dE for individual orbitals is unknown. For these cases, we employ a simple analytic form, which describes the shape of the df/dE curve of the ground-state hydrogen atom[20]

$$df/dw=N_{\rm ion}/(w+1)^2, \tag{6}$$

$$N_{\rm ion}=\int_0^\infty dw/(w+1)^2. \tag{7}$$

With this simplification, we get the binary-encounter-Bethe (BEB) model, which does not depend on any explicit knowledge of the *differential cross section*, df/dE. Instead, in terms of the *integrated* dipole quantity Q, we get the BEB cross section σ_Q per molecular orbital[20]

$$\sigma_Q=\frac{S}{t+u+1}\left[\frac{Q\ln t}{2}\left(1-\frac{1}{t^2}\right)+(2-Q)\left(1-\frac{1}{t}-\frac{\ln t}{t+1}\right)\right], \tag{8}$$

where $t=T/B$, $u=U/B$, $S=4\pi a_0^2N(R/B)^2$, a_0 is the Bohr radius, and R is the Rydberg energy.

We can simplify Eq. (8) further when Q is unknown by assuming $Q=1$, which has been shown to be an excellent approximation for many molecules.[21–25] By setting $Q=1$ in Eq. (5), one gets $m_{\rm ion}^2=NR/2B$ for individual molecular orbitals (MOs), and then $m_{\rm ion}^2$ can be summed over all MOs to get $M_{\rm ion}^2=\Sigma_{\rm MO}m_{\rm ion}^2$ for the molecule. The quantity $M_{\rm ion}^2$ plays an important role in the Bethe theory; it represents the leading term of the dipole contribution at high T, and can be extracted from experimental cross sections by using the Fano plot,[28] i.e., a plot of $\sigma_iT/4\pi a_0^2R$ versus $\ln(T/R)$. The slope of the Fano plot at high T is $M_{\rm ion}^2$. The theoretical value of $M_{\rm ion}^2=\Sigma m_{\rm ion}^2$ is, however, an asymptotic value that applies to σ_i at $T=\infty$ in principle. The values of $M_{\rm ion}^2$ empirically fitted at low or intermediate T are often higher than the theoretical limit. We shall return to this point in Sec. IV.

We denote the BEB cross section with $Q=1$ by $\sigma_{\rm BEB}$

$$\sigma_{\rm BEB}=\frac{S}{t+u+1}\left[\frac{\ln t}{2}\left(1-\frac{1}{t^2}\right)+1-\frac{1}{t}-\frac{\ln t}{t+1}\right]. \tag{9}$$

Note that Eq. (9) requires only B,U, and N for each molecular orbital in the ground state as the input. These constants can be determined using a molecular wave function code. The total ionization cross section σ_i is then simply the sum of $\sigma_{\rm BEB}$ over all occupied molecular orbitals

$$\sigma_i=\Sigma_{\rm MO}\,\sigma_{\rm BEB}. \tag{10}$$

B. Molecular wave functions

It is clear from Eq. (9) that $\sigma_{\rm BEB}$ and σ_i are determined by the molecular constants B,U, and N which in turn can be deduced from molecular wave functions. Based on applications to over 50 molecules,[29] we found that σ_i is most sensitive to the lowest value of B. To match the experimental cross sections near the lowest ionization threshold, it is necessary to use a realistic vertical ionization potential (IP). Hence, we use the experimental value of the first vertical IP, if available. With the exception of the first B value, all other parameters are determined using *ab initio* methods.

The actual values of the molecular constants needed depend on the level of approximation used. The self-consistent-field (SCF) method provides the simplest description of a molecular wave function. The kinetic energy U is determined directly as an expectation value. To get B, one can use orbital energies as an approximation, which is known as Koopmans' theorem.

When better accuracy is desired, one can calculate orbital binding energies by the so-called ΔSCF method, i.e., by taking the difference between the total energies of the parent molecule and the molecular ion with one electron removed from the desired orbital. Binding energies obtained by the ΔSCF method tend to be lower than those from Koopmans' theorem. Lower binding energies in turn make σ_i larger roughly by 10% at the peak in the cases we have studied, including the cross sections reported in this article. However, because a neutral molecule and its ion have different number of electrons, the difference in electron correlation energy sometimes causes the B values determined using the ΔSCF approach to be much smaller than the correct value. Because B must be deduced from the vertical IP, ion wave functions with the hole in various molecular orbitals must be determined using the same geometry as that for the parent molecule.

In the present work, we have used two types of molecular wave functions—the first type of wave functions are the SCF wave functions based on the restricted Hartree–Fock (RHF) method. Our past experience indicates that the cross sections calculated from RHF wave functions in general agree with experiments within $\pm 15\%$, and often are lower than experimental peak cross sections. The second type of wave functions are correlated wave functions of the complete-active-space (CAS) SCF type. In the following, we compare not only experimental and theoretical cross sections, but also cross sections from these two types of wave functions, labeled as RHF and CAS, to demonstrate the role of electron correlation in the BEB model.

C. Computational details of RHF wave functions

Following our previous practice,[21–25] we used the molecular structure code GAMESS[30] to calculate the RHF wave functions. Use was made of the standard basis sets available in GAMESS for expanding the molecular orbitals, as detailed below for each individual case.

(a) CF_4: Molecular orbitals were calculated with Gaussian 6-311+G(d) basis (i.e., with one d polarization function

TABLE II. Molecular orbital, electron occupation number N, orbital binding energy B, and orbital kinetic energy U calculated from the SCF and CAS wave functions for CF_4 and C_2F_6.

		B in eV		U in eV	
Orbital	N	RHF	CAS	RHF	CAS
		CF_4 T_d $^1A_1$			
$2a_1$	2	315.897	315.949	436.489	436.703
$3a_1$	2	49.6690	49.1356	87.7034	88.3200
$2t_2$	6	45.9274	45.7369	104.341	104.573
$4a_1$	2	27.6468	27.5325	87.8445	86.1408
$3t_2$	6	24.5365	24.2181	76.0006	75.2342
$1e$	4	20.9392	18.4791	83.4392	83.1922
$4t_2$	6	19.4262	17.8238	89.6581	89.1322
$1t_1$	6	16.20	16.20	95.5827	95.0687
	C_2F_6 D_{3d} $^1A_{1g}$				
$2a_{1g}$	2	314.466	314.564	436.293	436.281
$2a_{2u}$	2	314.450	314.550	436.501	436.528
$3a_{1g}$	2	49.2662	48.8989	87.7235	88.8204
$3a_{2u}$	2	48.5370	48.1615	93.3082	94.1643
$2e_u$	4	46.1614	46.0526	103.424	103.389
$2e_g$	4	45.8512	45.6036	106.259	107.038
$4a_{1g}$	2	30.0169	29.7421	69.9511	69.8403
$4a_{2u}$	2	26.8250	26.5610	84.5421	83.7481
$5a_{1g}$	2	25.2386	24.9773	66.9488	65.2726
$3e_u$	4	24.4005	24.1202	75.6263	74.2612
$3e_g$	4	23.5705	23.1705	77.9203	78.2997
$5a_{2u}$	2	21.1433	20.6861	83.6266	84.0259
$4e_g$	4	20.5609	20.8575	85.5065	82.1246
$4e_u$	4	20.4793	19.8235	86.2635	87.8509
$5e_u$	4	19.5187	18.4032	89.7359	88.5675
$5e_g$	4	18.9636	16.3618	94.5449	95.0405
$1a_{1u}$	2	18.8493	16.5564	94.5705	95.5036
$1a_{2g}$	2	18.6262	17.3921	96.4178	93.5362
$6a_{1g}$	2	14.48	14.48	81.8536	79.8863

and diffuse *s-p* functions on all atoms) and with the molecular symmetry group set as T_d.

(b) C_2F_6: Molecular orbitals were calculated with Gaussian 6-311+G(d) basis with the molecular symmetry group set as D_{3d} corresponding to the staggered conformation. The eclipsed conformation has a higher total energy as expected.

(c) C_3F_8: Many conformers are possible in principle because of the almost free rotation around the C–C bonds but the energy differences between the conformers are likely to be rather small. Also calculated orbital energies and the kinetic energies of the corresponding molecular orbitals in the different conformers are expected to be very close. Thus to minimize the computational resource requirement, the molecular symmetry group was assumed to be C_{2v} (i.e., the symmetry of the C–C–C backbone) and the Gaussian 6-311 basis set was used without any *d* polarization and diffuse *s-p* functions.

We present the values of the molecular orbital binding energies B (taken as negative of calculated orbital energies), kinetic energies U and electron occupation numbers N along with the symmetry character of the MOs for these molecules in Tables II and III.

In addition to the above calculations, SCF calculations using larger Gaussian basis, i.e., the correlated consistent triple-zeta and double-zeta basis of Dunning *et al.*[31] with augmented diffuse functions, have also been performed. However, for the purpose of consistency with our previous results, the cross sections labeled RHF here are calculated using the 6-311+G(d) or 6-311 basis set described above.

D. Computational details of CAS wave functions

In the second approach, we introduced correlation into the calculation of the molecular parameters. At first sight, it would appear that the BEB model is tailored to a SCF description of the target since the incoming electron interacts with the target electrons individually, with an implicit assumption that the remaining electrons are inactive. However, the sensitivity of σ_i to the use of an accurate first IP is an indication that correlation effects play a subtle role in the BEB model. Of the molecular parameters used in the calculation, B should be most susceptible to correlation effects since it includes a two-electron energy term. The kinetic energy U is an expectation value of a one-electron operator, hence making it insensitive to electron correlation, while the molecular orbital occupation numbers N are basically input data.

To incorporate electron correlation into B, we define

$$B_{\mathrm{corr}} = E_{\mathrm{ion}} - E_{\mathrm{mol}} = \mathcal{I}, \tag{11}$$

where E_{mol} is the total energy of the parent molecule and E_{ion} is the total energy of a particular ion state, both from

TABLE III. Molecular orbital, electron occupation number N, orbital binding energy B, and orbital kinetic energy U calculated from the SCF and CAS wave functions for C_3F_8 C_{2v} $^1A_1$.

		B in eV		U in eV	
Orbital	N	RHF	CAS	RHF	CAS
$3b_2$	2	316.055	315.032	436.390	436.505
$4a_1$	2	316.055	315.032	436.399	436.440
$5a_1$	2	314.433	313.334	436.260	436.355
$6a_1$	2	49.4023	48.4499	87.5595	89.2534
$4b_2$	2	49.0839	48.1642	90.9225	92.2343
$7a_1$	2	47.8703	47.0485	95.9562	97.1072
$3b_1$	2	46.5914	45.9056	102.393	103.384
$8a_1$	2	46.3791	45.7260	104.510	105.141
$2a_2$	2	46.3465	45.6825	105.218	105.845
$5b_2$	2	46.3410	45.6798	104.819	105.602
$4b_1$	2	46.0852	45.4376	106.329	106.828
$9a_1$	2	32.2373	31.2659	64.7472	64.0161
$6b_2$	2	29.1216	28.3788	70.3828	71.3995
$10a_1$	2	26.5883	26.1474	79.9208	78.5507
$7b_2$	2	25.3774	24.6590	66.2472	64.3508
$11a_1$	2	24.7188	24.1528	70.7535	70.0770
$5b_1$	2	24.3705	23.9025	73.2518	73.2541
$3a_2$	2	23.9270	23.4834	75.2014	75.1731
$12a_1$	2	23.6848	23.2059	74.9497	74.0686
$8b_2$	2	23.6331	23.1841	76.1494	75.7518
$6b_1$	2	22.4984	22.1718	78.5429	78.2293
$13a_1$	2	21.3392	20.8249	83.3914	82.1512
$9b_2$	2	21.1759	19.4751	85.2884	84.2002
$7b_1$	2	20.9174	19.9493	85.5409	84.0994
$14a_1$	2	20.6371	18.5926	87.6259	86.1235
$4a_2$	2	20.5337	19.1381	87.6816	85.9127
$10b_2$	2	20.4983	18.3131	88.1184	87.0845
$5a_2$	2	20.4630	17.9812	88.9676	87.7140
$8b_1$	2	19.7745	18.3167	89.6612	88.7050
$15a_1$	2	19.7310	18.1021	90.0537	89.4966
$9b_1$	2	19.5160	17.8834	93.3169	92.3058
$6a_2$	2	19.4425	17.6349	93.7631	93.2133
$11b_2$	2	19.3854	17.6208	93.2515	92.8540
$10b_1$	2	19.2820	14.9001	94.8657	94.4775
$7a_2$	2	19.2684	15.8598	95.7504	95.1908
$16a_1$	2	18.2752	15.1521	83.3675	81.6107
$12b_2$	2	13.70	13.70	81.4761	78.9048

correlated wave functions, while $\mathcal{I}$ is the ionization potential which produces that ion state. In using Eq. (11) care must be given to (a) the way electron correlation is introduced to E_{mol} and E_{ion} since the two systems have different number of electrons, and (b) the choice of ion states. In general a number of ion states of each symmetry are calculated, and E_{ion} are determined from ion states with a dominant configuration-state-function describing a hole state. Ion states arising from approximately equal mixtures of several hole states fall outside the description of the BEB model and are discarded. Also, B_{corr} are determined only for the valence electrons. For core electrons the B values are determined from the orbital energies of the RHF function calculated using the same Gaussian basis.

Symmetry breaking of the neutral and ionic states is another aspect to be considered. Because molecular calculations with Gaussian basis sets use the Abelian group instead of point group symmetry, molecular wave functions frequently are calculated using lower symmetry than its actual point group symmetry. For example, CF_4 belongs to the T_d point group but our CAS calculation used C_{2v} symmetry. The imbedded higher symmetry in the low symmetry calculation always guarantee the higher symmetry to be retained in the RHF wave function of the neutral molecule. In a correlated calculation, higher symmetry will be maintained only if the correlating orbitals are carefully chosen to span the proper symmetry correctly. If the set of correlating orbitals are too restricted, it often results in deviations from the higher symmetry. Symmetry breaking is often the rule in the calculation of ions. The problem arises because the equilibrium geometries of the ion states frequently are of lower symmetry and a variational calculation using the lower, C_{2v} symmetry gives lower energies than a corresponding calculation enforcing T_d symmetry. Thus the higher T_d symmetry will not be maintained unless the calculation is actually done in that symmetry. As a result, the ionization energies of the T_{2x}, T_{2y}, and T_{2z} orbitals are slightly different. To reconstitute the T_d symmetry, we enforced the same IP for the three degenerate orbitals T_{2x}, T_{2y}, and T_{2z}. The value of the IP was chosen to be the smallest of the three calculated IPs. The same procedure was used for other degenerate orbitals in CF_4 as well as for C_2F_6 and C_3F_8.

Complete-active-space SCF functions for the target and ion states have been calculated using the MOLPRO code.[32] For CF_4 the correlation-consistent aug-cc-pVTZ basis of Dunning and co-workers,[31] $[10s5p2d1f|4s3p2d1f]$ augmented with $1s1p1d1f$ diffuse functions, were used. For C_2F_6 and C_3F_8 the aug-cc-pVDZ basis, $[9s4p1d|3s2p1d]$ augmented with diffuse $1s1p1d$, were employed. All calculations were done using the experimental equilibrium geometry (see Sec. III C on the discussion of conformers for C_2F_6 and C_3F_8). In the case of CF_4, we correlated the outermost eight electrons in an active space of 12 orbitals. The corresponding ion states were calculated using the same active space but by correlating seven electrons. The *ab initio* value of the first vertical IP from the present calculation is 16.19 eV, versus an experimental value of 16.20 eV (Table I). For C_2F_6 and C_3F_8, the active space used varies with the symmetry of the ion state. For each ion state, a CAS calculation on the neutral molecule was always done using the same active space. For C_2F_6 the *ab initio* first vertical IP is 14.92 eV versus the experimental value of 14.48 eV (Table I). For C_3F_8, the *ab initio* value of 14.17 eV is to be compared with 13.70 eV from experiment (Table I). The increasing disagreement between theory and experiment for the first vertical IPs indicates the insufficient size of the active space as the molecules become larger.

To correct for the deficiencies in the CAS data for C_2F_6 and C_3F_8, a scale factor F_c is introduced. The use of a scale factor is a common practice in quantum chemistry calculations, particularly in the study of potential energy surfaces.[33] The constant F_c is defined to be equal to the difference between the CAS first IP and experimental first IP

$$F_c = \mathcal{I}_1(\mathrm{CAS}) - \mathcal{I}_1(\mathrm{expt}). \tag{12}$$

We then assume that the limited CAS introduces similar errors to all higher IPs. Thus the scaled ith IP is

$$\mathcal{I}_i(\mathrm{scaled\,CAS}) = \mathcal{I}_i(\mathrm{CAS}) - F_c. \tag{13}$$

For $i=1$, this adjustment forces the scaled CAS IP to be equal to the experimental first IP.

In Tables II and III, we compare the values of B and U calculated using RHF and CAS wave functions. All CAS B values, including those of CF_4, have been scaled as described above. Together with the values of N, the molecular constants in Tables II and III are sufficient to generate the BEB cross sections presented later for comparison to experimental data.

E. Multiple ionization

Another factor we must consider is multiple ionization. Electron-impact ionization of a molecule usually produces singly charged molecular ions and fragment ions as well as some multiply charged ions. Most experiments measure the ion current rather than the number of ions produced, e.g., the cross section for a doubly charged ion is multiplied by two, and so on. This is known as the *gross* ionization cross section. Although there is a distinct possibility for ejecting two or more electrons from the same orbital, this type of multiple ionization is common only in the valence shells of heavy atoms. For a molecule that consists of light atoms, a more likely mechanism is the Auger process in which an inner-shell hole is filled by a valence electron while the excess energy is dissipated by ejecting another electron from the same or an energetically nearby valence orbital. The resulting doubly charged molecular ion is unstable and eventually dissociates into two singly charged fragments.

On the other hand, most collision theories, including the BEB model, calculate the number of ionizing events known as the *counting* ionization cross section, making it difficult to compare such a theory directly to experimental data. To estimate the cross section for multiple ionization (or production of two molecular fragment ions from single ionizing collision), we have assumed that all holes generated in molecular orbitals with binding energies large enough to generate Auger electrons will decay through the Auger process, hence resulting in a doubly charged ion or two singly charged fragments. In either case, we can estimate the gross ionization cross section by doubling the BEB cross sections for some inner-shell orbitals. Since tightly bound inner-shell orbitals ($B>150$ eV) have very small ionization cross sections, we doubled cross sections only for those orbitals with 40 eV $<B<150$ eV.

Cross sections for multiple ionization estimated in this way increase the peak values by about 5% while shifting the peak slightly toward higher T. This shifting of the peak changes the shape of σ_i in a subtle way, but sufficient to improve the agreement in shape between theory and experiment for large molecules.[25]

F. Neutral dissociation

In its original formulation, the BEB theory assumes that all energy transfers *above a given orbital binding energy* will result in the ejection of an electron from either that orbital or other orbitals with lower binding energies. This is a general assumption used in most binary-encounter type theories for ionization. However, this assumption does not hold well for a molecule, since an energy transfer may result in the dissociation of the molecule into neutral fragments, such as $CF_4 \rightarrow CF_3+F$. As a result, the BEB theory counts neutral dissociation as ionization as long as the required energy for dissociation is higher than the lowest IP. On the other hand, the neutral dissociation cross sections, σ_{nd}, will not be counted in an experiment where ions or ejected electrons are detected. Hence, the BEB theory should be an upper limit to the total ionization cross section if a sufficiently accurate ground-state wave function is used. For many molecules, neutral dissociation via excited states below the lowest ionization threshold is dominant. However, the BEB theory *does not include neutral dissociation resulting from excitations to levels below the lowest IP*. In the BEB theory, an energy transfer is converted to a cross section appropriate for the ejection of an electron, rather than for neutral dissociation. Hence, there is no *a priori* reason for the excess cross section in the BEB theory to be numerically the same or proportional to the correct σ_{nd}. Nevertheless, as is shown in Sec. IV, we found surprising similarity in the cross section shape when we compared the difference between our experiment and the best BEB cross section to recent experimental σ_{nd} of CF_4 by Motlagh and Moore.[34] The exact relation between the excess BEB cross section and the correct σ_{nd} should be an interesting topic for further investigation.

IV. RESULTS AND DISCUSSION

Our experimental σ_i for CF_4, C_2F_6, and C_3F_8 are listed in Table IV with combined uncertainties from statistical and systematic effects. The electrometers used for the measurement of I_i and I_e were checked before and after the experiment with a standard resistance of 10^{12} ohm (relative standard uncertainty $\pm 0.5\%$). These electrometers showed no remarkable change in sensitivity. Electron energies were monitored with a voltage attenuator (relative standard uncertainty $\pm 2.5\%$). The relative standard uncertainty of the manometer in the measured range is $\pm 5.1\%$ of the reading according to the supplier. Extension of the effective electron path length due to the applied magnetic field and the drawout field is negligible. The purity of each target gas is 99.95% according to the supplier. Hence the uncertainty from the sample impurity is negligible.

As mentioned previously, electron intensity at the ion collection plate D2 (see Fig. 1) was given by $(I_{e1}+I_{e2})/2$. In the present study, the electron intensity I_{e2} slightly increases with increasing target gas pressure at $T>100$ eV. This is the reason why we did not choose I_{e1} as the incident electron intensity. Using the measured σ_i, more probable electron intensity $I_{e0}\exp(-n\sigma_i l)$ can be estimated at $l=4.3$ cm where I_{e0} is the electron intensity at $l=0$. For practical reasons, we chose $I_{e0}=I_{e1}$ and took the maximum value of σ_i for the target molecules. Then, the ratio of the two electron intensities $(I_{e1}+I_{e2})/2$ and $I_{e0}\exp(-n\sigma_i l)$ at D2 is estimated to be 98.2%, 97.1%, and 95.7% for CF_4, C_2F_6, and C_3F_8, respectively. These values give maximum deviation of measured electron intensities from the likely values at D2. The upper limits of the resultant uncertainties from systematic effects obtained by taking these values into consideration are, for $T<900$ eV and $T\geqslant 900$ eV: 5.5% and 6.1% for CF_4, 6.0%

TABLE IV. Total ionization cross sections (Å^2). Numbers in parentheses indicate combined relative standard uncertainty in percent owing to statistical and systematic effects.

T(eV)	CF_4	C_3F_8	T(eV)	C_2F_6
16	0.034(6.2)	0.129(7.4)		
17	0.080(6.2)	0.316(6.8)	17	0.0889(6.2)
18	0.137(5.7)	0.562(6.8)	18	0.211(6.5)
19	0.204(5.7)	0.815(6.8)	19	0.375(6.2)
20	0.295(5.6)	1.13(6.8)	21	0.782(6.3)
22	0.479(6.2)	1.81(6.8)	23	1.18(6.1)
24	0.656(6.4)	2.31(6.9)	25	1.59(6.3)
26	0.937(6.4)	3.08(6.8)	27	2.11(6.2)
28	1.19(5.8)	3.58(6.8)	29	2.49(6.2)
30	1.41(5.9)	4.10(6.8)	31	2.81(6.2)
32	1.62(6.0)	4.57(6.8)	33	3.16(6.1)
34	1.83(5.9)	5.12(6.7)	35	3.49(6.2)
36	2.03(7.5)	5.58(6.7)	37	3.86(6.0)
38	2.18(5.8)	5.88(6.8)	39	4.17(6.1)
40	2.38(5.7)	6.54(6.8)	41	4.54(6.2)
42	2.60(6.0)	7.01(6.8)	43	4.85(6.2)
44	2.78(5.9)	7.43(6.9)	45	5.14(6.2)
46	2.98(5.7)	7.85(6.8)	47	5.52(6.3)
48	3.25(5.7)	8.31(6.8)	49	5.77(6.3)
50	3.41(5.6)	8.99(6.8)	51	6.19(6.0)
60	3.97(5.5)	10.4(6.7)	61	6.82(6.2)
70	4.39(5.8)	11.3(6.8)	71	7.57(6.2)
80	4.76(5.9)	11.9(6.8)	81	7.84(6.3)
90	4.91(6.2)	12.5(7.0)	91	8.17(6.2)
100	5.12(5.7)	12.8(6.9)	101	8.39(6.0)
125	5.31(5.6)	13.3(6.7)	126	8.77(6.6)
150	5.28(5.6)	13.4(6.8)	151	8.75(6.0)
175	5.31(5.9)	13.2(6.9)	176	8.76(6.1)
200	5.10(5.7)	12.8(6.8)	201	8.57(6.4)
250	4.78(5.5)	12.1(6.8)	251	8.17(6.2)
300	4.59(5.6)	11.2(6.8)	301	7.41(6.1)
350	4.31(5.8)	10.5(7.0)	351	7.13(6.3)
400	4.05(6.1)	9.80(6.8)	401	6.55(6.4)
450	3.83(5.8)	9.31(6.8)	451	6.21(6.3)
500	3.51(5.8)	8.61(7.2)	501	5.89(6.5)
600	3.11(5.9)	7.80(6.7)	601	5.17(7.8)
700	2.83(5.7)	6.99(6.7)	701	4.72(6.6)
800	2.61(5.8)	6.41(6.8)	801	4.40(6.4)
900	2.38(6.2)	5.82(6.8)	901	3.96(6.3)
1000	2.23(6.3)	5.48(7.3)	1001	3.77(6.5)
1250	1.89(6.2)	4.64(7.3)	1251	3.19(6.7)
1500	1.64(6.3)	4.05(7.2)	1501	2.79(7.0)
1750	1.50(6.3)	3.62(7.2)	1751	2.44(6.6)
2000	1.34(6.3)	3.31(7.2)	2001	2.28(6.5)
2500	1.15(6.1)	2.78(7.3)	2501	1.88(6.5)
3000	0.990(6.4)	2.44(7.3)	3001	1.67(6.6)

and 6.5% for C_2F_6, and 6.7% and 7.2% for C_3F_8, respectively. The results for all molecules are compared with available data in Figs. 4–8.

In Fig. 4 we compare our theoretical and experimental σ_i for CF_4 with available experimental data,[1,6,9,10] all of which agree within the combined uncertainties. The cross section based on the ''DM formalism'' by Margreiter *et al.*[19] is also included in Fig. 4. The BEB cross section calculated from the RHF wave function appears to agree best with the present experiment, but the BEB cross section increases by ~5% when the CAS wave function is used. Moreover, multiple ionization discussed earlier (Sec. III E) increases the ionization cross section further. Since the BEB theory implicitly includes the neutral dissociation cross section σ_{nd}, the BEB cross section could be larger than experimental σ_i.

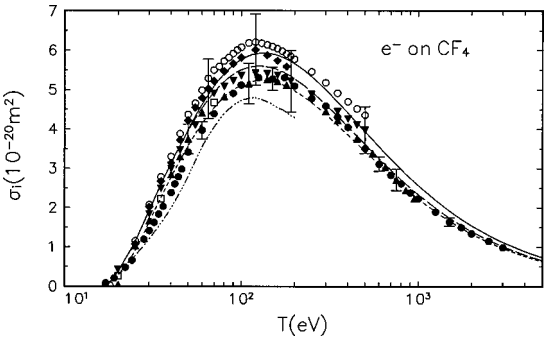

FIG. 4. Total ionization cross section σ_i for CF_4 vs incident energy T. Solid curve, present theoretical cross section from the CAS wave functions with estimates for multiple ionization; long dashed curve, present theoretical cross section from the CAS wave functions without estimates for multiple ionization; short dashed curve, present theoretical cross section from the RHF wave function without multiple ionization; dot–dashed curve, ''DM formalism'' cross section by Margreiter *et al.* (Ref. 19); filled circles, present experiment; diamonds, experimental data by Poll *et al.* (Ref. 6); inverted triangles, data by Bruce and Bonham (Ref. 9); upright triangles, data by Rao and Srivastava (Ref. 10); squares, data by Beran and Kevan (Ref. 1); and open circles, ''recommended'' cross section adopted by Christophorou *et al.* (Ref. 35).

We also included in Fig. 4 the total ionization cross section ''recommended'' by Christophorou *et al.*[35] as part of their comprehensive review of electron impact cross sections for CF_4. Their total ionization cross section is ~10% higher than our experiment at the peak. Since the present experimental cross section and that by Rao and Srivastava[10] were not yet available at the time of their review, their recommendation was influenced by the experimental data by Poll *et al.*[6] and the ionization data compiled by Bonham,[36] which are higher than any of the experimental data included in Fig. 4.

In Fig. 5, the excess BEB cross section obtained by taking the difference between the present experimental σ_i and the BEB cross section from the CAS wave function augmented by the multiple ionization cross section is compared to the recent experimental σ_{nd} by Motlagh and Moore,[34] who directly measured the production of neutral fragments from CF_4 by electron impact. There is a striking similarity in the T-dependence between the two sets of data. We also have

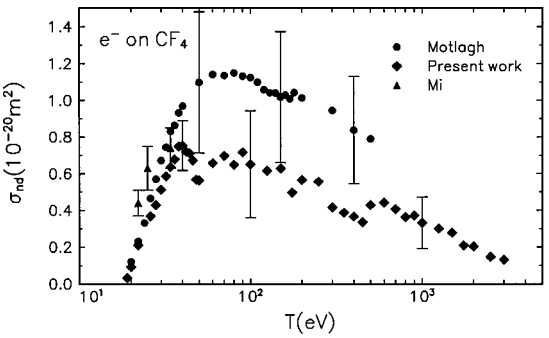

FIG. 5. Neutral dissociation cross section σ_{nd} for CF_4 vs incident energy T. Circles, experimental data by Motlagh and Moore (Ref. 34); diamonds, difference between the present theory and experiment; and triangles, experimental data by Mi and Bonham (Ref. 37).

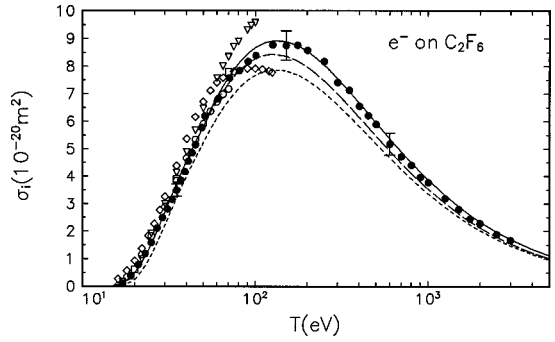

FIG. 6. Total ionization cross section σ_i for C_2F_6 vs incident energy T. Solid curve, present theoretical cross section from the CAS wave functions with estimates for multiple ionization; long dashed curve, present theoretical cross section from the CAS wave functions without estimates for multiple ionization; short dashed curve, present theoretical cross section from the RHF wave function without multiple ionization; filled circles, present experiment; squares, experimental data by Beran and Kevan (Ref. 1); diamonds, data by Poll and Meichsner (Ref. 5); inverted triangles, data by Kurepa (Ref. 3); and open circles, ''suggested'' cross section adopted by Christophorou and Olthoff (Ref. 40).

included a recent direct measurement of σ_{nd} by Mi and Bonham[37] in Fig. 5. The magnitude of their data are consistent with the two sets of data discussed above, though the range of T covered by Mi and Bonham is too narrow to determine the T-dependence of their data. The uncertainty in our excess BEB cross section is large because the leading part, σ_i, has been canceled in the subtraction. The three sets of data are consistent with each other when we take into account the uncertainties in both measured σ_{nd} and the excess BEB cross section. We also note that the σ_{td} measured by Winters and Inokuti[7] for CF_4 is about 5% higher than the present experimental σ_i at the peak, consistent with the fact that the former closely corresponds to $\sigma_i+\sigma_{nd}$ as was mentioned earlier.

Considering the additional uncertainty of the BEB theory itself, which could be as much as $\pm 15\%$, it is indeed surprising that a clear T-dependence can be seen. The peaking of σ_{nd} at $T\sim 80$ eV and a slow decline at higher T is characteristic of a dipole-allowed transition, suggesting that the neutral dissociation, which is dominated by the process $CF_4 \rightarrow CF_3+F$, takes place through excitations to dipole-allowed excited states. The large uncertainty in the numerical value of σ_{nd}, however, makes it difficult to extract the squared matrix element for neutral dissociation, M_{nd}^2 defined in analogy to M_{ion}^2 for total ionization, Eq. (4), by examining the high-T behavior of σ_{nd}.

A similar subtraction of the experimental σ_i by Rao and Srivastava[10] from our best BEB cross section leads to a cross section in good agreement with our excess BEB cross section at 100 eV$<T<$600 eV, but we infer from the shape of their cross section that the σ_i by Rao and Srivastava is too low at $T<100$ eV and too high at $T>600$ eV, although these deviations are still within the uncertainties ($\pm 10\%$) quoted for their σ_i. The direct measurement of σ_{nd} reported by Sugai *et al.*[38] is one order of magnitude smaller than the cross sections shown in Fig. 5, and peaks at $T=120$–130 eV.

In Figs. 6 and 7 we compare our theoretical and experimental results for C_2F_6 and C_3F_8 together with the experimental data by Beran and Kevan,[1] Kurepa,[3] and Poll and Meichsner,[5] respectively. For C_3F_8 in Fig. 7, we also included the experimental data by Chantry and Chen,[39] who directly measured the total ionization cross section. Agreement among the experiments for C_2F_6 is good at $T<70$ eV, although estimates of total uncertainty (ordinary random + systematic effects) are not available for the cited measurements. In the case of C_3F_8, the data by Beran and Kevan[1] and those by Poll and Meichsner[5] agree well with ours, while those of Kurepa[3] are considerably higher and those by Chantry and Chen[39] are the lowest. The total ionization cross section ''suggested'' by Christophorou and Olthoff[40] for C_2F_6 is in excellent agreement with the present experimental cross section (Fig. 6), while their ''suggested'' cross section[41] for C_3F_8 is $\sim 10\%$ lower than the present experimental result near the peak (Fig. 7). Unlike the case of CF_4, σ_{td} for C_2F_6 and C_3F_8 measured by Winters and Inokuti[7] are lower by 5%–10% than our experimental σ_i near the peak. No error limits are quoted by Winters and Inokuti and hence it is difficult to conclude whether these differences are significant or not.

For both molecules, the BEB cross sections obtained from the CAS wave functions seem to agree very well with the present experiment, contrary to the case for CF_4. This, however, is likely to be a fortuitous agreement caused by the use of CAS wave functions which are insufficiently correlated owing to the large number of bound electrons and the limited active space used. For instance, the quality of the CAS wave function we have used for C_2F_6 is likely to be better than that for C_3F_8. We can see a discernible trend that our best BEB cross section for C_3F_8 is slightly below the experiment, that for C_2F_6 is slightly above the experiment, and that for CF_4 is visibly above the experiment, directly corresponding to the electron correlation represented for each molecule. Hence, we expect the use of better correlated wave functions for C_2F_6 and C_3F_8 will eventually lead to BEB cross sections, when augmented by estimates for mul-

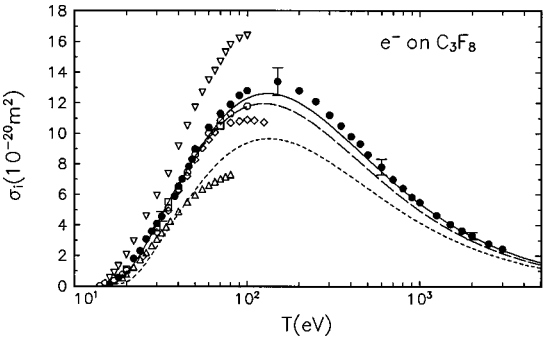

FIG. 7. Total ionization cross section σ_i for C_3F_8 vs incident energy T. Solid curve, present theoretical cross section from the CAS wave functions with estimates for multiple ionization; long dashed curve, present theoretical cross section from the CAS wave functions without estimates for multiple ionization; short dashed curve, present theoretical cross section from the RHF wave function without multiple ionization; filled circles, present experiment; squares, experimental data by Beran and Kevan (Ref. 1); diamonds, data by Poll and Meichsner (Ref. 5); upright triangles, data by Chantry and Chen (Ref. 39); inverted triangles, data by Kurepa (Ref. 3); and open circles, ''suggested'' cross section adopted by Christophorou and Olthoff (Ref. 41).

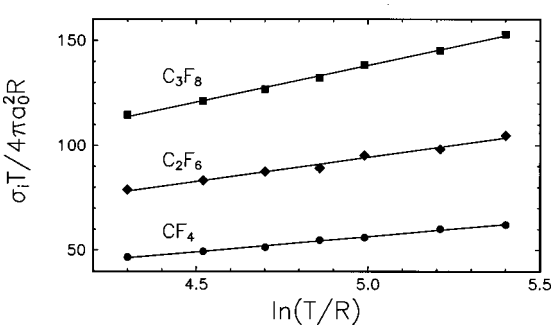

FIG. 8. Fano plot of the present experimental data.

TABLE V. $M^2_{\rm ion}$ for total ionization.

CF_4	C_2F_6	C_3F_8	Energy range (keV)	Source
14.6	23.1	35.1	1.0–3.0	Present work (exper.)
14.7	23.2	32.1	1.0–3.0	Present work (theory)
9.50	14.8	20.5	$T=\infty$	Present work (theory)
10.26			100–270	Ref. 42 (exper.)
10.3			$T=\infty$	Ref. 7 (exper., total inelastic)
19.2			0.2–0.6	Ref. 7 (exper., total dissoc.)
20.4			0.25–0.5	Ref. 8 (exper.)

tiple ionization, slightly higher than the measured σ_i, and allow us to explore possible links between experimental σ_{nd} and the excess BEB cross section as in CF_4.

Based on the Bethe theory, Fano[28] suggested a method, the so-called Fano plot, for obtaining the squared matrix element $M^2_{\rm ion}$ from the experimental results which include the total ionization process. Figure 8 shows the Fano plot of our σ_i measured at $T \geqslant 1$ keV. The experimental values of $M^2_{\rm ion}$ are listed in Table V. To date, three groups reported $M^2_{\rm ion}$ for the ionization of CF_4. Rieke and Prepejchal[42] measured ionization cross sections of many atoms and molecules including CF_4 for high energy (0.1–2.7 MeV) electrons and positrons. Their experimental value of $M^2_{\rm ion}$ for CF_4 was 10.26. Winters and Inokuti[7] obtained 19.2 from σ_{td} measured at $T=200$–600 eV. Ma *et al.*[8] deduced a value of 20.4 from σ_i measured at $T=250$–500 eV. On the other hand, Winters and Inokuti[7] obtained a value of 10.3 for the total inelastic collisions from photoabsorption cross sections, which include ionization. This is nearly equal to the experimental value for ionization reported by Rieke and Prepejchal.[42]

The numerical values of $M^2_{\rm ion}$ obtained as the slope of the straight line in the Fano plot (see Fig. 8) depend strongly on the range of T used. The general tendency is that the slope is smaller the higher the T. For instance, the $M^2_{\rm ion}$ value for CF_4 measured by Rieke and Prepejchal[42] at T between 100 and 270 keV is in excellent agreement with the BEB value (valid at $T=\infty$), while those determined at lower T are all higher (Table V). The theoretical value for the total inelastic scattering (i.e., ionization plus discrete excitations) by CF_4 reported by Winters and Inokuti[7] is somewhat higher than our BEB value as expected. If we deduce $M^2_{\rm ion}$ value for the BEB cross section by fitting the theoretical cross section between 1 and 3 keV, we reproduce the $M^2_{\rm ion}$ values fitted from the present experimental results as is shown in Table V. This trend clearly indicates that the asymptotic behavior predicted by the Bethe theory is reached at higher T than the incident energy range used by Winters and Inokuti, Ma *et al.*, and us.

Next we ask for the dependence of measured σ_i on the total number of electrons z in a molecule and the molecular polarizability α. In Table VI, σ_i/z, σ_i/α, and $\sigma_i/\sqrt{\alpha z}$ are shown for $T=0.1$–3 keV. We have used $\alpha(CF_4)=3.838\,\text{Å}^3$ and $\alpha(C_2F_6)=6.82\,\text{Å}^3$ to prepare Table VI.[43] The values of σ_i/α for C_3F_8 are not shown in the table because α for this molecule is not known well. As shown in Table VI, the values of σ_i/z and σ_i/α at low $T \leqslant 200$ eV are nearly constant, respectively. At each row in Table VI, the values of σ_i/z simply increase from left to right, while the values of σ_i/α show an opposite trend. On the other hand, the values of $\sigma_i/\sqrt{\alpha z}$ for CF_4 and C_2F_6 are nearly constant at each row (within 1%). If the values of $\sigma_i/\sqrt{\alpha z}$ obtained for CF_4 and C_2F_6 were applied to C_3F_8, we can estimate α for C_3F_8 to be $\alpha=10.6\,\text{Å}^3\pm0.8\,\text{Å}^3$. This value is close to the semiempirical value of $9.4\,\text{Å}^3$ calculated by Beran and Kevan[44] using the Lippincott-Stutman method without any bond polarity corrections. In the present work, σ_i includes a relative standard uncertainty component due to systematic effects of $\pm5.8\%$. Therefore the total relative standard uncertainty of our $\alpha(C_3F_8)$ value is estimated to be approximately $\pm7.3\%$.

One distinct advantage of the BEB model is that it provides a simple analytic expression for the ionization cross section that is valid from the threshold to several keV in T [see Eq. (9)]. Although its advantage is tempered somewhat by the large number of molecular orbital constants for C_3F_8 (Table III), we recommend the ''RHF'' constants for CF_4, and ''CAS'' constants for C_2F_6 and C_3F_8 for applications

TABLE VI. The ratio σ_i/z (Å^2), σ_i/α (Å^{-1}), and $\sigma_i/(z\alpha)^{1/2}$ (Å$^{1/2}$).

	CF_4			C_2F_6			C_3F_8
T(keV)	σ_i/z	σ_i/α	$\sigma_i/\sqrt{\alpha z}$	σ_i/z	σ_i/α	$\sigma_i/\sqrt{\alpha z}$	σ_i/z
0.1	0.122	1.33	0.403	0.127	1.23	0.395	0.142
0.2	0.121	1.32	0.402	0.130	1.26	0.404	0.144
0.4	0.0964	1.06	0.319	0.0992	0.96	0.309	0.109
0.6	0.074	0.81	0.245	0.0783	0.76	0.244	0.0867
0.8	0.0621	0.68	0.206	0.0667	0.65	0.207	0.0712
1.0	0.0531	0.58	0.176	0.0571	0.55	0.178	0.0609
2.0	0.0319	0.35	0.106	0.0345	0.33	0.107	0.0367
3.0	0.0235	0.26	0.0780	0.0253	0.24	0.0787	0.0271

where analytic formulas are needed to reproduce σ_i, such as in plasma modeling.

V. CONCLUSIONS

The total ionization cross sections for CF_4 published earlier[1,6,9,10] are in good agreement with the present measurement. The existing experimental data[1,3,5] are in good agreement with the present measurement on C_2F_6 from the threshold to $T \sim 70$ eV. On the other hand, the experimental data for C_3F_8 by Kurepa[3] are higher than our result, while the data by Chantry and Chen[39] are lower. The recommended/suggested total ionization cross sections adopted by Christophorou and co-workers[35,40,41] are slightly higher than the present experiment for CF_4, in excellent agreement for C_2F_6, and lower for C_3F_8.

The combination of reliable experimental σ_i with the BEB cross section obtained from correlated wave functions for CF_4 provided us with answers to several questions. First of all, electron correlation increases the BEB cross section, particularly between the threshold and the peak, reaching 5%–10% at the peak. We also found that the contribution from the Auger process initiated by inner-shell ionization increases σ_i by another ~5%.

The striking similarity in the T-dependence of directly measured σ_{nd} of CF_4 (see Fig. 5) and the excess BEB cross section obtained by subtracting the experimental σ_i from the BEB cross section calculated from correlated wave functions is a puzzle to us at present, because there is no rigorous theory to link σ_i to σ_{nd}. Further comparisons of the excess BEB cross sections to experimental data on directly measured σ_{nd}, for instance on CH_4 and SF_6, will be useful in understanding this puzzle.

Our best BEB cross sections for C_2F_6 and C_3F_8 are in excellent agreement with the present measurement. However, we consider this somewhat fortuitous in view of the situation seen in CF_4. We find a trend indicating that, were we to use better correlated wave functions, the theory would exceed the experimental σ_i. We find that electron correlation may increase BEB cross sections by as much as ~20% for a molecule with a large number of bound electrons, such as C_3F_8, although multiple ionization is unlikely to exceed ~5% of σ_i.

For molecules composed of the same chemical elements and bound by the same kind of chemical bonds, their optical oscillator strengths are distributed in similar excitation energy range. Only in such cases, the total number of bound electrons z and the molecular polarizability α will act as good parameters for scaling σ_i at sufficiently high T. In the present work, our empirical scaling using $\sqrt{\alpha z}$ showed surprisingly good results. Such a result encourages us to predict $\alpha = 10.6\ \text{Å}^3 \pm 0.8\ \text{Å}^3$ for C_3F_8. An independent confirmation of this empirical α is desirable.

Finally, the molecular orbital constants in Tables II and III together with Eq. (9) provide analytic formulas to express total ionization cross sections from threshold to several keV in T, which will facilitate the application of the present theory to modeling of plasma processing of semiconductor chips.

ACKNOWLEDGMENTS

We thank Dr. M. V. V. S. Rao and Professor J. Moore for providing us with their experimental results prior to publication. The work in Japan was partly supported by the cooperative program of the National Institute for Fusion Science and the work at NASA Ames was supported by the IPT on device/process modeling and nanotechnology. The work at NIST was supported in part by the Office of Fusion Energy Sciences, U. S. Department of Energy.

[1] J. A. Beran and L. Kevan, J. Phys. Chem. **73**, 3866 (1969).
[2] K. Stephan, H. Deutsch, and T. D. Märk, J. Chem. Phys. **83**, 5712 (1985).
[3] M. V. Kurepa, 3rd Cz. Conference on Electronics and Vacuum Transactions (1965).
[4] J. T. Tate and P. T. Smith, Phys. Rev. **39**, 270 (1932).
[5] H. U. Poll and J. Meichsner, Contrib. Plasma Phys. **27**, 5,359 (1987).
[6] H. U. Poll, C. Winkler, D. Margreiter, V. Grill, and T. D. Märk, Int. J. Mass. Spectrom. Ion Processes **112**, 1 (1992).
[7] H. F. Winters and M. Inokuti, Phys. Rev. A **25**, 1420 (1982).
[8] C. E. Ma, M. R. Bruce, and R. A. Bonham, Phys. Rev. A **44**, 2921 (1991).
[9] M. R. Bruce and R. A. Bonham, Int. J. Mass Spectrom. Ion Processes **123**, 97 (1993).
[10] M. V. V. S. Rao and S. K. Srivastava, XXth International Conference on the Physics of Electronic and Atomic Collisions, Abstract Mo 150. Edited by F. Aumayr, G. Betz, and H. P. Winter, July 1997, Vienna, Austria.
[11] D. Rapp and P. Englander-Golden, J. Chem. Phys. **43**, 1464 (1965).
[12] N. F. Mott, Proc. R. Soc. London, Ser. A **126**, 259 (1930).
[13] H. Bethe, Ann. Phys. (Leipzig) **5**, 325 (1930).
[14] W. F. Miller, Ph.D. thesis, Purdue Univ. 1956 (unpublished).
[15] L. Vriens, in *Case Studies in Atomic Physics, Vol. I,* edited by E. W. McDaniel and M. R. C. McDowell (North Holland, Amsterdam, 1969), p. 335.
[16] P. Khare, Planet. Space Sci. **17**, 1257 (1969).
[17] Y.-K. Kim, Radiat. Res. **61**, 21 (1975); **64**, 205 (1975).
[18] D. K. Jain and S. P. Khare, J. Phys. B **9**, 1429 (1976).
[19] D. Margreiter, H. Deutsch, M. Schmidt, and T. D. Märk, Int. J. Mass Spectrom. Ion Processes **100**, 157 (1990).
[20] Y.-K. Kim and M. E. Rudd, Phys. Rev. A **50**, 3954 (1994).
[21] W. Hwang, Y.-K. Kim, and M. E. Rudd, J. Chem. Phys. **104**, 2956 (1996).
[22] Y.-K. Kim, W. Hwang, N. M. Weinberger, M. A. Ali, and M. E. Rudd, J. Chem. Phys. **106**, 1026 (1997).
[23] M. A. Ali, Y.-K. Kim, W. Hwang, N. M. Weinberger, and M. E. Rudd, J. Chem. Phys. **106**, 9602 (1997).
[24] Y.-K. Kim, M. A. Ali, and M. E. Rudd, J. Res. Natl. Inst. Stand. Technol. **102**, 693 (1997).
[25] Y.-K. Kim and M. E. Rudd, Comments At. Mol. Phys. **34**, 293 (1999).
[26] H. Nishimura and H. Tawara, J. Phys. B **27**, 2063 (1994).
[27] M. B. Robin, *Higher Excited States of Polyatomic Molecules* (Academic, New York, 1974), Vol. I, p. 180.
[28] U. Fano, Phys. Rev. **95**, 1198 (1954).
[29] Most of these molecular cross sections, updated references, and molecular constants included in Refs. 20–25 are available on a NIST website: http://physics.nist.gov/ionxsec
[30] M. W. Schmidt, K. K. Baldridge, J. A. Boatz, S. T. Elbert, M. S. Gordon, J. H. Jensen, S. Koseki, N. Matsunaga, K. A. Nguyen, S. J. Su, T. L. Windus, M. Dupuis, and J. A. Montgomery, J. Comput. Chem. **14**, 1347 (1993).
[31] T. H. Dunning, J. Chem. Phys. **90**, 1007 (1989); R. A. Kendall, T. H. Dunning, and R. J. Harrison, *ibid.* **96**, 6796 (1992).
[32] MOLPRO 96 is a package of *ab initio* programs written by H.-J. Werner and P. J. Knowles, with contributions from J. Almlöf, R. D. Amos, M. J. O. Deegan, S. T. Elbert, C. Hampel, W. Meyer, K. Peterson, R. Pitzer, A. J. Stone, and P. R. Taylor.
[33] H. Partridge and D. W. Schwenke, J. Chem. Phys. **106**, 4618 (1997).
[34] S. Motlagh and J. H. Moore, J. Chem. Phys. **109**, 432 (1998).
[35] L. G. Christophorou, J. K. Olthoff, and M. V. V. S. Rao, J. Phys. Chem. Ref. Data **25**, 1341 (1996).
[36] R. A. Bonham, Jpn J. Appl. Phys., Part I **33**, 4157 (1994).

[37] L. Mi and R. A. Bonham, J. Chem. Phys. **108**, 1910 (1998).
[38] H. Sugai, H. Toyoda, T. Nakano, and M. Goto, Contrib. Plasma Phys. **35**, 415 (1995).
[39] P. J. Chantry and C. L. Chen, J. Chem. Phys. **90**, 2585 (1989).
[40] L. G. Christophorou and J. K. Olthoff, J. Phys. Chem. Ref. Data **27**, 1 (1998).
[41] L. G. Christophorou and J. K. Olthoff, J. Phys. Chem. Ref. Data **27**,889 (1998).
[42] F. F. Rieke and W. Prepejchal, Phys. Rev. A **6**, 1507 (1972).
[43] T. M. Miller, in *Handbook of Chemistry and Physics*, 77th ed. (CRC, Boca Raton, FL, 1996-1997), p. **10**-199.
[44] J. A. Beran and L. Kevan, J. Phys. Chem. **73**, 3860 (1969).